Although the LCA was likely to have been a metabolically sophisticated respiratory organism[2,5,12], earlier more primitive microorganisms might also have had the capacity to transfer electrons to extracellular Fe(III). The evolution of this metabolic capability would have provided organisms with an energetic advantage over early fermentative microorganisms by greatly expanding the range and extent of potential electron-donor oxidation. Once reduced, iron can readily transfer electrons to other electron acceptors, and this may have led to the intracellular incorporation of Fe(III)/Fe(II) redox couples that are common in more complex, modern electron-transport pathways. □

Methods

Organisms were obtained from the Deutsche Sammlung von Mikroorganismen und Zellkulturen (DSMZ). For studies with cell suspensions, cells were grown in the medium suggested by the DSMZ for their cultivation. Cells were collected by centrifugation under N_2–CO_2 (80:20), and washed cell suspensions were prepared in anaerobic bicarbonate buffer (30 mM; pH 6.8) to provide ~0.1 mg of cell protein in 5 ml bicarbonate buffer under N_2–CO_2. H_2 (101 kPa) was added as the electron donor and Fe(III) citrate (5 mM) was added as the electron acceptor. For studies on the growth of *P. islandicum* with Fe(III), cells were grown in DSMZ medium 390 in which thiosulphate and sodium sulphide had been replaced by Fe(III) citrate (15 mM) as the electron acceptor and 0.25 mM cysteine as a sulphur source, with 0.02% yeast extract added. H_2 was provided at 101 kPa; the incubation was done at 90 °C. For studies on the growth of *T. maritima* with Fe(III), cells were grown in TB medium[25] modified by substituting PIPES buffer with bicarbonate (30 mM), decreasing the cysteine to 0.5 mM, adding 0.05% yeast extract, and supplying H_2 (101 kPa) and Fe(III) citrate (15 mM); incubation was at 80 °C. For growth on Fe(III) oxide, organisms were grown on the media described but with Fe(III) citrate replaced with 100 mM Fe(III) oxide[26]. Cell numbers were monitored with acridine orange staining and epifluorescent microscopy[27]. Production of Fe(II) was quantified with ferrozine[26].

Received 15 April; accepted 1 July 1998.

1. Madigan, M. T., Martinko, J. M. & Parker, J. *Biology of Microorganisms* (Prentice Hall, Upper Saddle River, New Jersey, 1997).
2. Pace, N. R. Origin of life—facing up to the physical setting. *Cell* **65,** 531–533 (1991).
3. Adams, M. W. W. Enzymes and proteins from organisms that grow near and above 100 °C. *Annu. Rev. Microbiol.* **47,** 627–658 (1993).
4. Stetter, K. O. Hyperthermophilic procaryotes. *FEMS Microbiol. Rev.* **18,** 149–158 (1996).
5. de Duve, C. *Vital Dust* 1–362 (Basic Books, New York, 1995).
6. Walker, J. C. G. Was the Archaean biosphere upside down? *Nature* **329,** 710–712 (1987).
7. Cairns-Smith, A. G., Hall, A. J. & Russell, M. J. Mineral theories of the origin of life and an iron sulfide example. *Orig. Life Evol. Biosph.* **22,** 161–180 (1992).
8. Walker, J. C. G. & Brimblecombe, P. Iron and sulfur in the pre-biologic ocean. *Precambr. Res.* **28,** 205–222 (1985).
9. Kasting, J. F. Earth's early atmosphere. *Science* **259,** 920–926 (1993).
10. De Ronde, C. E. J., De Wit, M. J. & Spooner, E. T. C. Early Archean (<3.2 Ga) Fe-oxide-rich, hydrothermal discharge vents in the Barberton greenstone belt, South Africa. *Geol. Soc. Am. Bull.* **106,** 86–104 (1984).
11. Holm, N. G. Why are hydrothermal systems proposed as plausible environments for the origin of life? *Origins Life Evol. Biosphere* **22,** 5–14 (1992).
12. Barns, S. M. & Nierzwicki-Bauer, S. A. Microbial diversity in ocean, surface, and subsurface environments. *Rev. Mineral.* **35,** 35–79 (1997).
13. Lonergan, D. J. *et al.* Phylogenetic analysis of dissimilatory Fe(III)-reducing bacteria. *J. Bacteriol.* **178,** 2402–2408 (1996).
14. Lovley, D. R., Coates, J. D., Saffarini, D. A. & Lonergan, D. J. in *Iron and Related Transition Metals in Microbial Metabolism* (eds Winkelman, G. & Carrano, C. J.) 187–215 (Harwood, Switzerland, 1997).
15. Boone, D. R. *et al. Bacillus infernus* sp. nov., an Fe(III)- and Mn(IV)-reducing anaerobe from the deep terrestrial subsurface. *Int. J. Sys. Bacteriol.* **45,** 441–448 (1995).
16. Slobodkin, A., Reysenbach, A.-L, Strutz, N., Dreier, M. & Wiegel, J. *Thermoterrabacterium ferrireducens* gen. nov., sp. nov., a thermophilic anaerobic dissimilatory Fe(III)-reducing bacterium from a continental hot spring. *Int. J. System. Bacteriol.* **47,** 541–547 (1997).
17. Greene, A. C., Patel, B. K. C. & Sheehy, A. J. *Deferribacter thermophilus* gen. nov., sp. nov., a novel thermophilic manganese- and iron-reducing bacterium isolated from a petroleum reservoir. *Int. J. System. Bacteriol.* **47,** 505–509 (1997).
18. Liu, S. V. *et al.* Thermophilic Fe(III)-reducing bacteria from the deep subsurface: the evolutionary implications. *Science* **277,** 1106–1109 (1997).
19. Lovley, D. R., Stolz, J. F., Nord, G. L. & Phillips, E. J. P. Anaerobic production of magnetite by a dissimilatory iron-reducing microorganism. *Nature* **330,** 252–254 (1987).
20. Lovley, D. R. in *Iron Biominerals* (eds Frankel, R. B. & Blakemore, R. P.) 151–166 (Plenum, New York, 1990).
21. McKay, D. S. *et al.* Search for past life on Mars: possible relic biogenic activity in Martian meteorite ALH84001. *Science* **273,** 924–930 (1996).
22. Gold, T. The deep, hot biosphere. *Proc. Natl Acad. Sci. USA* **89,** 6045–6049 (1992).
23. Huber, R. *et al. Thermotoga maritima* sp. nov. represents a new genus of unique extremely thermophilic eubacteria growing up to 90 °C. *Arch. Microbiol.* **144,** 324–333 (1986).
24. Ravot, G. *et al.* Thiosulfate reduction, an important physiological feature shared by members of the order *Thermotogales*. *Appl. Environ. Microbiol.* **61,** 2053–2055 (1995).
25. Childers, S., Vargas, M. & Noll, K. M. Improved methods for cultivation of the extremely thermophilic bacterium *Thermotoga neapolitana*. *Appl. Environ. Microbiol.* **58,** 3949–3953 (1992).
26. Lovley, D. R. & Phillips, E. J. P. Organic matter mineralization with reduction of ferric iron in anaerobic sediments. *Appl. Environ. Microbiol.* **51,** 683–689 (1986).
27. Hobbie, J. E., Daley, R. J. & Jasper, S. Use of Nuclepore filters for counting bacteria by fluorescence microscopy. *Appl. Environ. Microbiol.* **33,** 1225–1228 (1977).

Acknowledgements. This work was supported by a grant from the LExEN program of the NSF.

Correspondence and requests for materials should be addressed to D.R.L. (e-mail: dlovley@microbio.umass.edu).

The role of nonlinear dynamics of the syrinx in the vocalizations of a songbird

Michale S. Fee*, Boris Shraiman*, Bijan Pesaran† & Partha P. Mitra*

* *Bell Laboratories, Lucent Technologies, 600 Mountain Avenue, Murray Hill, New Jersey 07974, USA*

† *Physics Department, California Institute of Technology, Pasadena, California 91125, USA*

Birdsong is characterized by the modulation of sound properties over a wide range of timescales[1]. Understanding the mechanisms by which the brain organizes this complex temporal behaviour is a central motivation in the study of the song control and learning system[2–8]. Here we present evidence that, in addition to central neural control, a further level of temporal organization is provided by nonlinear oscillatory dynamics that are intrinsic to the avian vocal organ. A detailed temporal and spectral examination of song of the zebra finch (*Taeniopygia guttata*) reveals a class of rapid song modulations that are consistent with transitions in the dynamical state of the syrinx. Furthermore, *in vitro* experiments show that the syrinx can produce a sequence of oscillatory states that are both spectrally and temporally complex in response to the slow variation of respiratory or syringeal parameters. As a consequence, simple variations in a small number of neural signals can result in a complex acoustic sequence.

Zebra-finch songs are organized into short segments of sound, referred to as syllables, that often contain rapid sequences of whistled notes, harmonic stacks and aperiodic signals[9,10]. Sounds within a syllable are produced contiguously with no silent interval during the transitions between distinct signal types (Fig. 1a). This continuity allows one to observe changes in the oscillatory state of the syrinx during modulations of the acoustic signal. We recorded the directed song of male zebra finches ($n = 12$) in a sound-isolation chamber. Close examination of the song spectra and acoustic waveforms shows sudden transitions from periodic to aperiodic or chaotic dynamics, period doubling, and mode-locking transitions. We believe that these features arise because the syrinx behaves as a low-dimensional nonlinear dynamical system.

Most (10 of 12) of the songs we recorded contained syllables exhibiting rapid (<10 ms) transitions from periodic to chaotic, or noisy, signals. Figure 1b shows two examples of this behaviour at an expanded timescale. These transitions sometimes occur in less than 1 ms, and often appear to jump back and forth between the periodic and chaotic oscillation. Another characteristic of nonlinear dynamical systems, period doubling, is characterized by a change in oscillation frequency such that spectral components appear at half the original frequency spacing. An example of period doubling in zebra-finch song is shown in Fig. 1c; at the time marked with the asterisk (*), note the rapid onset of interspersed harmonic components as described above. Period-doubling transitions were seen in three of the zebra-finch songs examined.

Zebra-finch song syllables can also exhibit modulations that suggest the presence of mode locking in the syringeal dynamics.

Mode locking occurs when two components of a system are constrained by some nonlinear interaction to maintain a small integer ratio of oscillation frequencies. If the characteristic frequency of one component of the system is changed relative to the other, mode-locking transitions may occur as the oscillation frequency suddenly jumps to achieve a new stable integer ratio with the fixed frequency[11,12]. In zebra-finch song, for example, syllables often exhibit[10] an overall downward sweep in fundamental frequency. However, this downward frequency sweep may be punctuated by steps, or rapid transitions in fundamental frequency (Fig. 1c). In the example shown, the mode-locking transitions occur such that the oscillation frequency maintains a ratio of two, three and four with respect to a common frequency at ~3 kHz. Similar features were observed in 9 of the 12 zebra-finch songs studied.

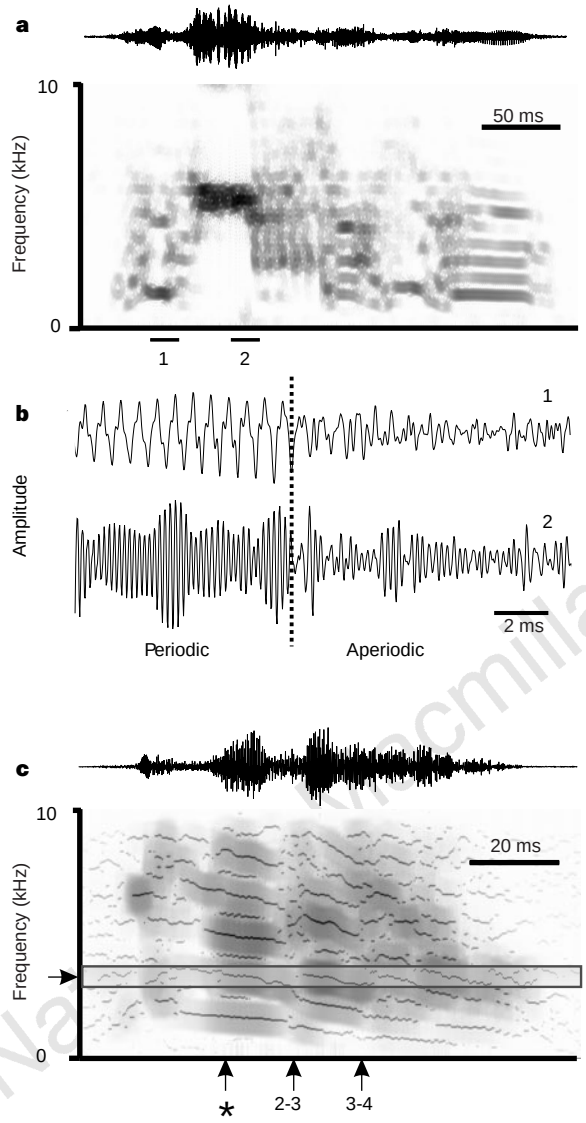

Figure 1 Spectral and temporal characteristics of zebra-finch song. **a**, The spectrogram of a syllable displaying the wide variety of spectral features common in zebra-finch song, such as a high-frequency nearly sinusoidal signal, broadband aperiodic signals, and periodic signals characterized by harmonic stacks. The pressure waveform is shown at the top. **b**, The rapid transitions between these signals are seen by expanding the pressure waveform around the regions marked 1 and 2 in **a**. In both cases, note that the transition from a nearly periodic signal to a noisy signal occurs in roughly 1 ms. **c**, Spectrogram and harmonic analysis of a syllable recorded from a different bird. The spectrogram is shown superimposed with the result of a harmonic analysis in which sinusoids are fit to the signal in the same time window on which the spectra were computed. Note the rapid frequency-doubling transition at the time marked with the asterisk. The overall downward sweep in the fundamental frequency of this syllable is marked by a series of jumps, or sudden transitions. A rapid transition in oscillation frequency occurs at the point marked (2–3) such that the third harmonic after the transition has approximately the same frequency as the second harmonic before the transition. Approximately 15 ms later, another transition occurs such that the fourth harmonic is suddenly shifted down to the frequency of the third harmonic. The second, third and fourth harmonic in this sequence are all roughly aligned with the bright spectra band at 3,200 Hz, indicated by the horizontal bar and arrow.

We suggest two hypotheses for the origin of the song features described above: direct muscular manipulation during singing of the syringeal parameters by the song control system, or alternatively, intrinsic dynamics of the syrinx. To distinguish between these hypotheses, we examined the acoustic signals generated by an *in vitro* preparation of the zebra finch syrinx ($n = 6$). The excised syrinx was induced to oscillate by applying suction at the trachea and pressure at the bronchial inlet. *In vitro* oscillations of the zebra-finch syrinx were quite similar in oscillation frequency and amplitude to normal zebra-finch song and occurred over a range of pressures and flow rates that was physiologically reasonable[13]. Spectra of the sound signals measured outside the syrinx (Fig. 2a) show an enhancement of lower harmonics compared with normal song spectra. The high harmonic components in song are thought to be produced by the rapid pressure fluctuations associated with closure of the bronchial lumen during syringeal oscillation; we expect that such rapid fluctuations would be relatively suppressed in the sound signal measured outside the syrinx.

A smooth ramp-down and ramp-up of air pressure applied at the tracheal outlet produced a sequence of oscillatory states, typically with jumps in oscillation frequency and, at higher pressures, transitions from periodic to aperiodic oscillation (Fig. 2a). The precise sequence of acoustic signals produced during this manipulation was different for each preparation. The acoustic sequence was also sensitive to small changes in various experimental parameters, such as tension on the bronchus. Intrinsic differences in syringes and sensitivity to parameters may partly account for some variations across individuals and variability within individuals, respectively. Another feature that was commonly observed was hysteresis in the acoustic signal; the sequence of acoustic signals generated as the pressure was ramped up usually differed in a repeatable manner from the sequence as the pressure was ramped down. The transitions observed during this manipulation were usually abrupt, often occurring in approximately one period of the acoustic signal (Fig. 2b).

Further evidence for nonlinear dynamics of the syrinx was seen during simple manipulations of syringeal configuration. Deflection of the labium externum (LE) (Fig. 3) into the bronchial lumen constricts the flow of air through the syrinx, and is thought to be a normal articulation during song production[14]. In all of the syringes tested ($n = 3$), this constriction resulted in a large increase in the fundamental oscillation frequency during *in vitro* oscillation. However, in two syringes the frequency was not a smooth function of LE displacement; rather the frequency exhibited sudden jumps at certain discrete displacements (Fig. 2c). Furthermore, the oscillation seems to be constrained to frequencies that are close to a small-integer sub-harmonic of a common (higher) frequency. In the example shown, the frequency jumps from ~700 Hz to ~1,100 Hz to ~2,200 Hz, which have periods, approximately, of three, two and one times the period of the common 2,200-Hz component, respectively.

To understand the origin of the apparent strong nonlinearity in the syrinx, we used a stroboscopic imaging technique to visualize *in vitro* oscillations of the zebra-finch syrinx ($n = 5$) (Fig. 3). *In vitro*, there was a threshold flow rate (~0.5 standard litres per minute) at which the labium internum (LI) and the medial tympaniform membrane (MTM) began to oscillate with large amplitude motion (~0.5 mm). The motion of these membranes was phase-locked to each other and to the generated sound, suggesting that

these membranes are in fact the source of the sound. In all syringes studied, the anatomical structure exhibiting the largest motion amplitude was the LI, rather than the much lighter MTM, which agrees with recent evidence that the LI plays a central role in syrinx function[15]. Close examination of the strobed oscillation under a microscope indicated that the bronchial lumen is probably closed briefly by contact of the LI with the LE during part of the oscillatory cycle; however, the wave-like motion of the medial membranes made it difficult to determine quantitatively the fraction of time during the oscillation that the bronchial lumen was closed. Because the excursions of these membranes are comparable to the size of the bronchial lumen, the Bernoulli forces driving the oscillation[16] are a highly nonlinear function of membrane displacement.

To determine if our stroboscopic and acoustic observations of *in vitro* syringeal oscillations are consistent with a view of the syrinx as a nonlinear dynamical system, we developed a biophysical model of the syrinx. We followed previous work on both human[17] and avian[16] vocalizations, as well as models of fluid flow through collapsible

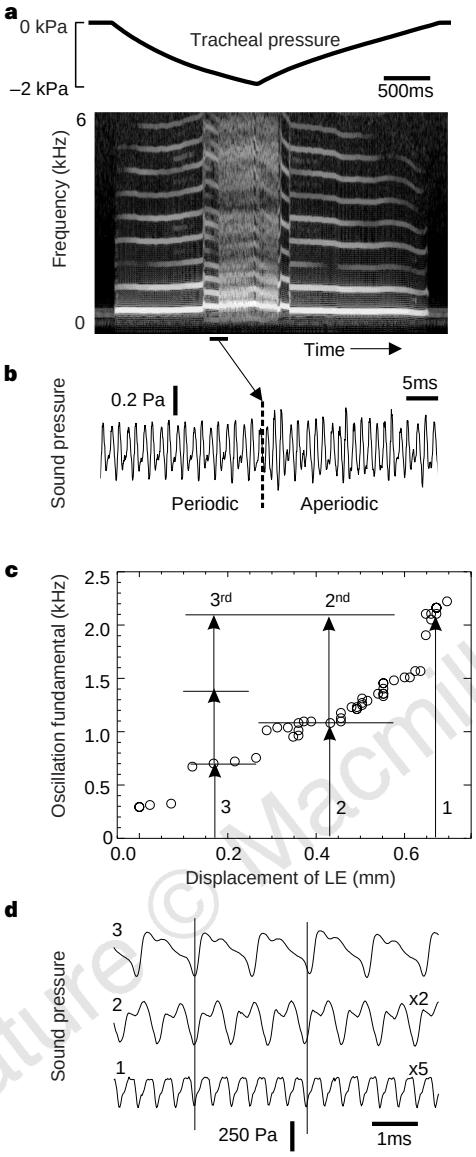

Figure 2 Patterns of acoustic signals generated in the *in vitro* syrinx preparation during slow modulation of syringeal and flow parameters. Application of suction to the trachea and slight over-pressure to one bronchus results in sustained oscillation of the ipsilateral syringeal membranes. **a**, As the tracheal pressure (top) is varied over a range of 2 kPa, the sound generated by syrinx exhibits a sequence of modulations in fundamental frequency, including period doubling, as well as a transition from periodic oscillation to broadband, apparently chaotic oscillations. Bronchial pressure is held constant (0.4 kPa). The sound is recorded outside the syrinx, ~2 cm from the MTM. **b**, Examination of the pressure signal around the transition from periodic to chaotic oscillation shows that the transition occurs in approximately one oscillatory period. **c**, Displacement of the third bronchial ring (and thus the LE) into the bronchial lumen increases the fundamental oscillation frequency over a range of nearly three octaves before the oscillation ceases. As a function of LE displacement, the fundamental frequency exhibits a series of discrete jumps. In this example, the third harmonic, second harmonic and fundamental are roughly aligned with a common frequency at ~2.2 kHz. **d**, Acoustic waveform measured at labial displacements indicated in **c**. Note the entrainment of the oscillation fundamental to three, two and one period(s) of the high-frequency component. The three waveform segments are shown at different scales, as indicated. The sound was recorded inside the trachea with a probe microphone.

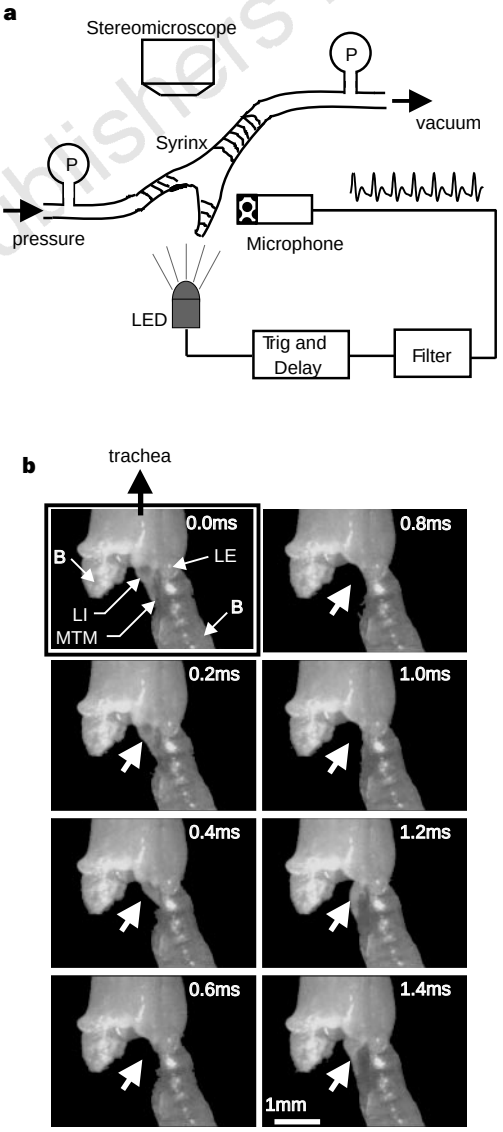

Figure 3 Stroboscopic observation of *in vitro* syringeal oscillations. **a**, Experimental setup. The syrinx is induced to oscillate *in vitro* by applying suction to the trachea and slight overpressure to one bronchial tube. The sound pressure measured ~2 cm from the syrinx is used to trigger an array of bright LEDs with a variable time delay. **b**, The configuration of the medial tympaniform membrane (MTM) and labium internum (LI) was visualized and recorded as the time delay was slowly swept through several oscillation periods. The digitized video frames are shown at increments of 0.2 ms in the time delay. In this case the oscillation frequency was ~700 Hz. Note that both the MTM and LI exhibit a large amplitude of motion. Also labelled are the labium externum (LE) and bronchi (B).

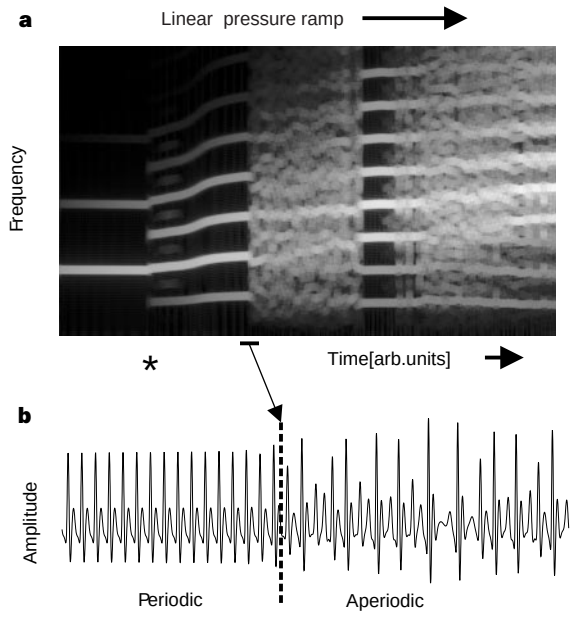

Figure 4 Results of a simple numerical model of airflow through a compliant constriction. The syringeal membranes are modelled as a system of coupled masses and springs. **a**, Spectrogram of the oscillatory membrane displacement. The parameter associated with bronchial pressure is ramped slowly and linearly up from zero. Note the period doubling events (asterisk), and the rapid transition to 'chaotic' dynamics. **b**, The membrane displacement shown expanded around the latter transition showing that the transition occurs rapidly, that is, in approximately one oscillatory period.

tubes[18]. The model is formed by a set of ordinary differential equations describing the mechanical motion of the syringeal membranes in the presence of airflow through the bronchial tube. The essential nonlinearity in the model is the nonlinear pressure-flow relation associated with the Bernoulli force. The membranes were modelled as a two-mass system. Membrane parameters were based on estimates of the resonant mode structure of the LI and the MTM (M.S.F. and P.P.M., unpublished results). The essential result is that the model exhibits qualitatively similar behaviour to *in vivo* zebra-finch song as well as the *in vitro* syringeal oscillations. The model shows period doubling and transitions from periodic to chaotic dynamics (Fig. 4), as well as mode-locking transitions (not shown). Our model results suggest a mechanism for the observed mode locking, namely coupling of the basic Bernoulli oscillation to a higher vibrational mode in the membranes. An additional mechanism that might underlie mode locking is the coupling of the oscillatory mechanism to tracheal resonances.

The generic signatures of nonlinear dynamics described here have also been described in models of human vocalizations[19], and in patients with vocal disorders[20]. A distinction with human vocalizations demonstrated by our model and the *in vitro* results is that detailed spectral shaping in zebra-finch song arises in large part from syringeal dynamics[1], as opposed to filtering effects of the vocal tract.

We have demonstrated that the isolated syrinx behaves as a classic nonlinear dynamical system, often exhibiting rapid transitions between distinct oscillatory states. The nonlinear behaviour of the zebra-finch syrinx results from the large amplitude motion of the vibrating membranes and the involvement of the relatively heavy LI. As a consequence, simple trajectories in a small number of control parameters can result in a complex sequence of acoustic signals. Thus, in addition to the central song control system, the syrinx must also be viewed as an important component in the hierarchy of structures determining the temporal organization of birdsong. Furthermore, the resulting complexity of the mapping from articulators to acoustic output suggests that song learning may require a sophisticated internal model of syringeal dynamics. □

Methods

Isolated syrinx. Adult male zebra finches (Canary Bird Farm, Old Bridge, New Jersey) were anaesthetized and killed by decapitation. The syrinx was removed, cleaned of excess connective tissue, and mounted in the experimental chamber. The trachea was connected to an adjustable vacuum source, and one bronchial tube was connected to a source of humid air with adjustable pressure. The other bronchial tube was pinched closed and sealed with cyanoacrylate. The trachea and anterior portion of the syrinx was embedded in 3% agarose in 10 mM phosphate-buffered saline. Tracheal and bronchial pressures were recorded with electronic pressure sensors (Sensym). Above a threshold flow rate (~0.5 standard litres per minute), the LI and the MTM oscillated spontaneously over a wide range of flow rates (0.5–2.5 standard litres per minute) and pressure differentials between the trachea and bronchus (0.1–2.0 kPa). Oscillation at pressures or flow rates higher than this physiological range resulted in rupture of the medial membranes. Acoustic signals generated by the syrinx were recorded using either an electret microphone placed ~2 cm from the syrinx, or with a probe microphone (Etymotic Research) placed into the trachea.

Syrinx response to parameter changes. Dependence of the oscillatory state of the excised syrinx on parameters was examined for variations in both tracheal pressure and membrane tension. To study pressure variations, the bronchial inlet was held at a constant pressure (0–0.5 kPa) while the tracheal outlet pressure was smoothly ramped down 1–2 kPa below atmospheric pressure, and then ramped back to atmospheric pressure. The control pressures were measured ~50 cm from the syrinx to reduce the sensitivity of the pressure measurement to changes in syringeal resistance. The dependence of oscillatory state on the position of the LE was examined during sustained syringeal oscillation at a constant tracheal pressure. By using forceps, the LE was forced manually into the bronchial lumen until the oscillation ceased. Simultaneous video recording of the preparation and the acoustic signal enabled later quantification of LE displacement and the associated acoustic modulations. Displacement of the LE produced no apparent displacement or tensioning of the LI or MTM, so the frequency changes were probably a result purely of constriction of the bronchial lumen, rather than tension changes.

Stroboscopic imaging. Stroboscopic images of the oscillating syrinx were obtained *in vitro* to examine in detail the motion of the LI and the MTM. The syrinx was induced to oscillate as described above. Pulsed illumination (10 μs duration) from a cluster of four bright light-emitting diodes (LEDs) was synchronized with the fundamental oscillation period of the membrane as follows. The measured acoustic signal was rectified, band-pass filtered around the oscillation frequency (typically 500–1,000 Hz), and used to trigger a variable-delay pulse generator. The pulse generator triggered the LEDs at a known time relative to the acoustic signal. The delay was slowly swept through several milliseconds to sample all phases of the oscillation; the images were recorded with a CCD camera and video-recorded with a Sony Betacam recorder for later analysis.

Spectral analysis. Spectrograms were computed with direct multitaper spectral estimates[21]. In Fig. 1c, superimposed on the spectrogram is the F-spectrum[21]. This quantity measures the goodness-of-fit to a sinusoid at any given frequency. The F-spectrum was computed with a moving window, and the spectral components exceeding a fixed confidence level were superimposed on the displayed spectrogram.

Received 8 May; accepted 29 June 1998.

1. Greenewalt, C. H. *Brid Song: Acoustics and Physiology* (Smithsonian Institution Press, Washington DC, 1968).
2. Nottebohm, F., Stokes, T. M. & Leonard, C. M. Central control of song in the canary, *Serinus canarius*. *J. Comp. Neurol.* **165,** 457–486 (1976).
3. Nottebohm, F., Kelley, D. B. & Paton, J. A. Connections of vocal control nuclei in the canary telencephalon. *J. Comp. Neurol.* **207** (1982).
4. McCasland, J. S. Neuronal control of bird song production. *J. Neurosci.* **7,** 23–39 (1987).
5. Scharff, C. & Nottebohm, F. A comparative study of the behavioral deficits following lesions of various parts of the zebra finch song system: implications for vocal learning. *J. Neurosci.* **11,** 2896–2913 (1991).
6. Konishi, M. Pattern generation in birdsong. *Curr. Opin. Neurobiol.* **4,** 827–831 (1994).
7. Vu, E., Mazurek, M. E. & Kuo, Y.-C. Identification of a forebrain motor programming network for the learned song of zebra finches. *J. Neurosci.* **14,** 6924–6934 (1994).
8. Yu, A. & Margoliash, D. Temporal hierarchical control of singing in birds. *Science* **273,** 1871–1875 (1996).
9. Immelman, K. in *Bird Vocalizations* (ed. Hinde, R. A.) pp. 61–74 (Cambridge Univ. Press, 1969).

10. Price, P. H. Developmental determinants of structure in zebra finch song. *J. Comp. Physiol. Psychol.* **93,** 260–277 (1979).
11. Fletcher, N. H. Mode locking in non-linearly excited inharmonic musical oscillators. *J. Acoust. Soc. Am.* **64,** 1566–1569 (1978).
12. Jackson, E. A. *Perspectives of Nonlinear Dynamics* (Cambridge Univ. Press, 1992).
13. Hartley, R. S. & Suthers, R. A. Airflow and pressure during canary song: direct evidence for mini-breaths. *J. Comp. Phys. A* **165,** 15–26 (1989).
14. Goller, F. & Suthers, R. A. Implications for lateralization of bird song from unilateral gating of bilateral motor patterns. *Nature* **373,** 63–66 (1995).
15. Goller, F. & Larsen, O. N. A new mechanism of sound generation in songbirds. *Proc. Natl Acad. Sci. USA* **94,** 14787–14791 (1997).
16. Fletcher, N. H. Bird song—a quantitative acoustic model. *J. Theor. Biol.* **135,** 455–481 (1988).
17. Ishizaka, K. & Flanagan, J. L. Synthesis of voiced sounds from a two-mass model of the vocal cords. *Bell Syst. Tech. J.* **51,** 1233–1268 (1972).
18. Bertram, C. D. & Pedley, T. J. A mathematical model of unsteady collapsible tube behaviour. *J. Biomech.* **15,** 39–50 (1982).
19. Berry, D. A., Herzel, H., Titze, I. R. & Krischer, K. Interpretation of biomechanical simulations of normal and chaotic vocal fold oscillations with empirical eigenfunctions. *J. Acoust. Soc. Am.* **95,** 3595–3604 (1994).
20. Herzel, H., Berry, D. A., Titze, I. R. & Saleh, M. Analysis of vocal disorders with methods from nonlinear dynamics. *J. Speech Hear. Res.* **37,** 1008–1019 (1994).
21. Thompson, D. J. Spectrum estimation and harmonic analysis. *Proc. IEEE* **70,** 1055–1096 (1982).

Acknowledgements. We thank W. Denk, M. Konishi and S. S.-H. Wang for comments on the manuscript.

Correspondence and requests for materials should be addressed to M.S.F. (e-mail: fee@lucent.com).

When temporal terms belie conceptual order

Thomas F. Münte*‡, Kolja Schiltz* & Marta Kutas*†

** Department of Cognitive Science and † Department of Neurosciences, University of California, San Diego, La Jolla, California 92093-0515, USA*
‡ Department of Neurology, Medizinische Hochschule Hannover, 30623 Hannover, Germany

We conceive of time as a sequential order of real-world events, one event following another from past to present to future. This conception colours the way we speak of time ("we look forward to the time") and, as we show here, the way we process written statements referring to the temporal order of events, in real time. Terms such as 'before' and 'after' give us the linguistic freedom to express a series of events (real or imaginary) in any order. However, sentences that present events out of chronological order require additional discourse-level computation. Here we examine how and when these computations are carried out by contrasting brain potentials across two sentence types that differ only in their initial word ('After' X, Y versus 'Before' X, Y). At sites on the left frontal scalp, the responses to 'before' and 'after' sentences diverge within 300 ms; the size of this difference increases over the course of the sentences and is correlated with individual working-memory spans. Thus, we show that there are immediate and lasting consequences for neural processing of the discourse implications of a single word on sentence comprehension.

There is no common agreement of how conceptual knowledge in long-term memory (LTM) is used to create a mental representation of a sentence during online comprehension. However, there is a consensus that we create a temporary representation of a sentence and the situation it refers to[1–3]. In addition, words must activate world knowledge, although when this occurs remains controversial[1–3]. To examine this, we contrasted event-related brain potentials (ERPs) during the reading of two sentence types whose processing we expected to differ based on the linguistic and conceptual knowledge activated by their initial words ('before/after').

Both sentence types consist of an initial subordinate clause and a subsequent main clause, each describing a distinct event that is neither logically nor causally related to the other (for example, 'Before/After' the psychologist submitted the article, the journal changed its policy). In other words, the event in each clause could easily be understood without reference to the other. However, we believe that the first word leads readers to expect some non-arbitrary relationship between the two events. This expectation is based on real-world knowledge of time, and linguistic knowledge of how these notions map onto expressions of time. Our experiences in the real world suggest to us that time unfolds sequentially, with current events sometimes causing future events. Our linguistic knowledge tells us that temporal conjunctions often draw attention to the sequence of events in a discourse[4,5]. Moreover, 'before' and 'after' access such a sequence from different starting points: 'after'

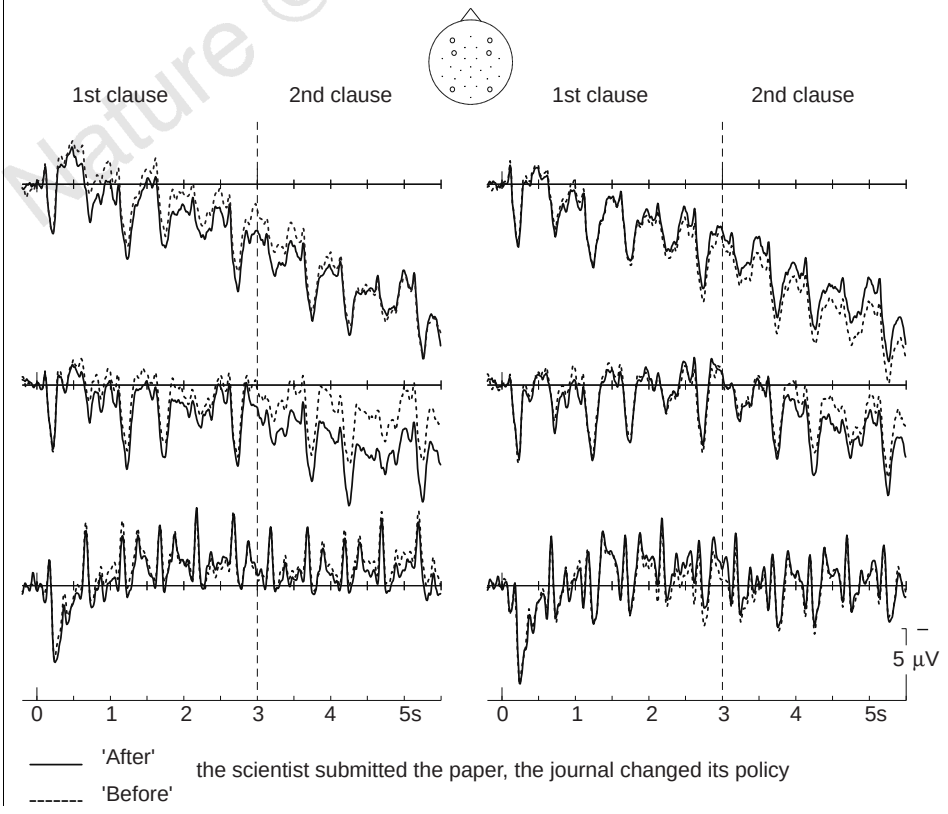

Figure 1 Grand average ($n = 24$) cross-sentence ERPs from prefrontal, frontal and occipital scalp sites (open circles on schematic head) of the left and right hemispheres (left and right sides of the figure, respectively) time-locked to 'before' or 'after'. 'Before' sentences are more negative than 'after' sentences throughout (main effect of sentence type: clause 1, $F_{1,23} = 9.98$, $P < 0.005$; clause 2, $F_{1,23} = 11.23$, $P < 0.003$), especially over the left compared with the right hemisphere sites (sentence type by site by hemisphere interaction: clause 1, $F_{10,230} = 4.63$, $P < 0.001$; clause 2, $F_{10,230} = 5.65$, $P < 0.001$). The difference between sentence types is reliably larger during the second than the first clause (main effect of clause for 'before/after' difference: $F_{1,23} = 4.78$, $P < 0.04$).